Atmos. Chem. Phys. Discuss., 15, 21803–21835, 2015
www.atmos-chem-phys-discuss.net/15/21803/2015/
doi:10.5194/acpd-15-21803-2015

Atmospheric Chemistry and Physics Discussions

Seasonality of ultrafine and sub-micron aerosols and the inferences on particle formation processes

H. C. Cheung[1], C. C.-K. Chou[1], M.-J. Chen[1], W.-R. Huang[1], S.-H. Huang[1], C.-Y. Tsai[1], and C. S.-L. Lee[2]

[1]Research Center for Environmental Changes, Academia Sinica, Taipei 11529, Taiwan
[2]Institute of Occupational Medicine and Industrial Hygiene, College of Public Health, National Taiwan University, Taipei, Taiwan

Received: 24 June 2015 – Accepted: 22 July 2015 – Published: 12 August 2015

Correspondence to: C. C.-K. Chou (ckchou@rcec.sinica.edu.tw)

Published by Copernicus Publications on behalf of the European Geosciences Union.

Abstract

The aim of this study is to investigate the seasonal variations in the physicochemical properties of atmospheric ultrafine particles (UFPs, $d \leq 100$ nm) and submicron particles (PM_1, $d \leq 1$ µm) in an East-Asian urban area, which are hypothesized to be affected by the interchange of summer and winter monsoons. An observation experiment was conducted at the TARO, an urban aerosol station in Taipei, Taiwan, from October 2012 to August 2013. The measurements included the mass concentration and chemical composition of UFPs and PM_1, as well as the particle number concentration (PNC) and size distribution (PSD) with size range of 4–736 nm. The results indicate that the mass concentration of PM_1 was elevated during cold seasons with peak level of 18.5 µg m^{-3} in spring, whereas the highest UFPs concentration was measured in summertime with a seasonal mean of 1.62 µg m^{-3}. Moreover, chemical analysis revealed that the UFPs and PM_1 were characterized by distinct composition; UFPs were composed mostly of organics, whereas ammonium and sulfate were the major constituents in PM_1. The seasonal median of total PNCs ranged from 13.9×10^3 cm^{-3} in autumn to 19.4×10^3 cm^{-3} in spring. The PSD information retrieved from the corresponding PNC measurements indicates that the nucleation mode PNC (N_{4-25}) peaked at 11.6×10^3 cm^{-3} in winter, whereas the Aitken mode (N_{25-100}) and accumulation mode ($N_{100-736}$) exhibited summer maxima at 6.0×10^3 and 3.1×10^3 cm^{-3}, respectively. The shift in PSD during summertime is attributed to the enhancement in the photochemical production of condensable organic matter that, in turn, contributes to the growth of aerosol particles in the atmosphere. In addition, remarkable photochemical production of particles was observed in spring and summer seasons, which was characterized with averaged particle growth and formation rates of 4.3 ± 0.8 nm h^{-1} and 1.6 ± 0.8 cm^{-3} s^{-1}, respectively. The prevalence of new particle formation (NPF) in summer is suggested as a result of seasonally enhanced photochemical oxidation of SO_2, which contributes to the production of H_2SO_4, and low level of PM_{10} ($d \leq 10$ µm) that serves as the condensation sink. Regarding the sources of aerosol particles, correla-

ACPD
15, 21803–21835, 2015

tion analysis upon the PNCs against NO_x revealed that the local vehicular exhaust was the dominant contributor of the UFPs throughout a year. On the contrary, the Asian pollution outbreaks can have significant influence in the PNC of accumulation mode particles during the seasons of winter monsoons. The results of this study underline the significance of secondary organic aerosols in the seasonal variations of UFPs and the influences of continental pollution outbreaks in the downwind areas of Asian outflows.

1 Introduction

Due to the significant impact of particulate matter on human health and climate change, it is vital to understand the formation process of atmospheric particles (Charlson et al., 1992; Donaldson et al., 1998). A number of mechanisms have been proposed by which atmospheric particles are formed, including binary nucleation, ternary nucleation and ion-induced nucleation for charged particles, under different environment conditions (Kulmala, 2003; Kulmala et al., 2004). Numerous studies have been conducted in different locations to elucidate particle formation processes under various environmental settings in the free troposphere, boreal forest and coastal areas, where new particles formation processes are observed frequently (Lee et al., 2008; O'Dowd et al., 1999; Weber et al., 2001; Vehkamäki 2004). Recently, investigations were also carried out on new particle formation within urban boundary layer (e.g., Cheung et al., 2013 and references therein), where particle formation was suggested to be mainly influenced by the photo-oxidation of SO_2. Furthermore, formation of particulate matter by heterogeneous reactions of gases on dust particles was reported (Hsu et al., 2014; Nie et al., 2012). Previous investigations have indicated that the air pollutants, both in gaseous and particulate form, associated with the continental outflows of air masses could have affected a wide region in East Asia and caused severe regional air pollution (e.g., Lin et al., 2004; Wang et al., 2003). However, the formation processes of ultrafine particles (UFPs, $d \leq 100$ nm) and sub-micron particles (PM_1, $d \leq 1$ µm) under the influences of continental outflows are not yet well understood.

ACPD
15, 21803–21835, 2015

In urban environment, major contributing sources of aerosol particles include the vehicular exhausts (e.g., Pey et al., 2008; Pérez et al., 2010), industrial emissions (Gao et al., 2009) and new particle formation by photochemical reactions (e.g., Pey et al., 2009). Approximately 55–69 % of the total particle number concentrations (PNCs) were attributed to secondary aerosols during midday in several European cities (Reche et al., 2011). In a subtropical urban area, Cheung et al. (2013) observed that there have been a ten-fold increase in nucleation mode PNCs (N_{9-25}, with size $9 < d < 25$ nm) compared to that contributed by the vehicle emission in Taipei, Taiwan. Besides the local sources, air quality of the East Asian countries is also strongly affected by the transport of air pollutants from mainland China during periods of winter monsoons (Cheung et al., 2005; Lin et al., 2004; Matsumoto et al., 2003). Lin et al. (2004) reported that the mass concentration of particulate matter (PM_{10}) due to the long-range transport associated with winter monsoons was 85 $\mu g\,m^{-3}$, about 79 % higher than that due to local pollution ($\sim 47.4\,\mu g\,m^{-3}$) in urban Taipei. Chemical composition of fine and coarse particles was measured during a winter monsoon period at Rishiri Island, near the northern tip of Japan, to study the transport of continental aerosols (Matsumoto et al., 2003). The results showed that higher levels of particle mass concentrations were associated with the outbreaks of continental polluted air masses. In addition, Cheung et al. (2005) found deterioration in visibility around the southern China during wintertime as indicated by a two-fold increase in aerosol light scattering coefficient under the influences of winter monsoons. All these studies were limited to measurements in terms of PM_{10} or $PM_{2.5}$ for a particular period, and the seasonality of particles in either ultrafine or sub-micron range has not been well illustrated yet.

To attain a better understanding of the seasonal variations of ultrafine and sub-micron particles and the factors affecting particle formation, particularly under the influences of Asian monsoon circulations, we conducted a 1 year aerosol characterization experiment in Taipei, Taiwan, a typical subtropical urban area in East Asia. In this study, we analyzed number concentration and size distribution of aerosol particles, together with the mass concentration and chemical composition of UFPs and PM_1 measured

ACPD
15, 21803–21835, 2015

during four seasonal campaigns (i.e. 24 October–15 November 2012, 4–24 January, 17 March–11 April, and 1–14 August 2013). The results of this study will contribute to the management strategies of the severe air pollution over the East Asia region.

2 Methodology

2.1 Observation site and instrumentation

The measurements were conducted at the Taipei Aerosol and Radiation Observatory (TARO, 25.02° N, 121.53° E), which locates in the downtown area of Taipei, Taiwan, during October 2012 to August 2013. The measurements were carried out for 2–3 weeks in each season (see Table 1 for measurement details). The aerosol observatory is on the top floor of the Building-B of the Department of Atmospheric Sciences, National Taiwan University (ASNTU), which is ~ 20 m a.g.l. (Cheung et al., 2013).

Particle size distribution (PSD) in the range of 4–736 nm was measured by two scanning mobility particle sizer (SMPS) systems. One was equipped with a long-differential mobility analyzer (long-DMA, Model: TSI 3081, TSI Inc.) and a condensation particle counter (CPC) (Model: TSI 3022A, TSI Inc.) to measure the particles from 10–736 nm, which was named long-SMPS. Another one was equipped with a nano-DMA (Model: TSI 3085, TSI Inc.) and an ultrafine water-based CPC (UWCPC, Model: TSI 3786, TSI Inc.) for measuring the particles from 4–110 nm, which was named nano-SMPS. The poly-disperse particles were classified into selected mono-disperse particles according to their electrostatic mobility by the DMAs. The number concentration of the mono-disperse particles was then counted by the CPCs. Ambient air was drawn into the SMPS systems from outside the building through a 0.635 cm (inner diameter) conductive tube, and a sampling duration of 5 min was adopted for each PSD measurement. The SMPS systems' flow rates were checked weekly during the sampling period and the accuracy of the particle sizing of the DMAs was checked using polystyrene

ACPD
15, 21803–21835, 2015

latex spheres (PSLs) before the campaigns. Operation details are referred to Cheung et al. (2013).

Size segregated aerosol samples were collected by a pair of Micro-Orifice Uniform Deposition Impactors (MOUDI, Model: 110, MSP Corp.). Taking the advantage that the cut diameter of the 10th MOUDI impaction stage is exactly 100 nm, the 11th impaction stage (cut diameter = 56 nm) of each MOUDI was removed to allow the after filter function as a collector of UFPs. Besides, a pair of PM_1 samplers, each consisted of a standard aerosol sampler (PQ-200, BGI Inc.) and a PM_1 sharp cut cyclone, were deployed to collect PM_1 samples. For both UFPs and PM_1 sampling arrangements, one of the paired samplers was equipped with Teflon filters, whereas another was equipped with quartz fiber filters. The Teflon filter samples were used for gravimetric measurement. The quartz filter samples were deployed for analysis of soluble ions (Na^+, NH_4^+, K^+, Ca^{2+}, Mg^{2+}, PO_4^{3-}, Cl^-, NO_3^-, SO_4^{2-}) using ion chromatograph (IC), and carbonaceous components (i.e. OC and EC) in the aerosols using a DRI-2001A carbonaceous aerosol analyzer with IMPROVE-A protocol. Details of the in-lab analysis are as described previously (Salvador and Chou, 2014). Both the PM_1 and UFPs were collected with double-layered quartz filters (i.e. QBQ setup) and the artifacts due to adsorption of gaseous components were corrected as suggested by Subramanian et al. (2004). The sampling duration of each sample set was from 14:00–12:00 LT (22 h), and a total of 69/75 sets of UFPs/PM_1 samples were collected during the entire investigation period (Autumn 20/21 sets, Winter 15/16 sets, Spring 25/25 sets and Summer 9/13 sets).

Moreover, to assist the data interpretation, the hourly averaged mass concentration of PM_{10}, the mixing ratio of trace gases (i.e. NO_x, SO_2 and O_3) and the meteorology parameters (i.e. wind direction/speed and UVB) from the Guting air quality station of Taiwan Environmental Protection Agency, which is about 1 km from the TARO, were analyzed in this study.

ACPD
15, 21803–21835, 2015

2.2 Data processing and analysis

The PSD of 4–736 nm presented in this study was combined from two sets of SMPS data, where the nano-SMPS corresponded to the size range of 4–49.6 nm, and the long-SMPS corresponded to the size > 49.6 nm. The diffusion loss of the particles during the sample transport in the tubing was corrected according to the algorithm proposed by Holman (1972). Particle number concentrations for different size ranges were then calculated from the SMPS measurements.

The 5 min PSD data were synchronized into hourly averages, and fitted by the DO-FIT model developed by Hussein et al. (2005) according to the multiple log-normal distribution algorithms. Based on the fitted PSD data, the PNCs were classified into $4 \le d \le 25$ nm (N_{4-25}), $25 \le d < 100$ nm (N_{25-100}), $4 \le d \le 100$ nm (N_{4-100}), $100 \le d < 736$ nm ($N_{100-736}$) and $4 \le d \le 736$ nm (N_{4-736}), for nucleation mode, Aitken mode, ultrafine, accumulation mode and total particles, respectively. Pearson correlation coefficient, r, was calculated by PASW Statistics ver. 18 (SPSS Inc.) to determine the correlation between the respective parameters.

2.3 Back-trajectory analysis

Backward trajectories were calculated using the HYSPLIT model (Hybrid Single Particle Lagrangian Integrated Trajectory, Version 4.9) of NOAA (National Oceanic and Atmospheric Administration) (Draxler, 1999) for TARO during the sampling period, in order to trace the origins of the air masses. Note that the grid resolution of the meteorological data used for back-trajectories calculation is $1^\circ \times 1^\circ$, which is not enough to trace the detailed air mass passage over the scale of the study region and, therefore, the trajectories only provide an indication of the region from which the air mass was originated.

As mentioned above, the air quality of urban Taipei is significantly affected by both the local vehicular exhausts and long-range transport of pollution, where the later one is dominated by meteorological factors. The information on the meteorological condi-

ACPD
15, 21803–21835, 2015

tions, particularly the wind patterns, is important and thus presented here. The back-trajectories of the air masses for the TARO are illustrated in Fig. 1 (left panel). The results showed that northeasterly winds were dominating in autumn and winter seasons, passing through the Asian continent before reaching Taiwan, whereas southerly winds were prevailing in summer that passed through the Taiwan Island. The air masses observed in spring period were found to be mainly associated with Asian continental outflows and occasionally with the southerly flows. This observation agreed with the surface wind direction measured in urban Taipei area (see Fig. 1, right panel), where northeasterly winds were dominating during the period from November 2012 to May 2013, and southerly winds were prevailing from May 2013 to August 2013.

3 Results and discussions

3.1 PNCs and PSDs in respective seasons

The PNCs of various size ranges during each season are summarized in Table 1. Relatively higher N_{4-736} were observed in spring and winter with median concentrations of 17.4×10^3 and 19.4×10^3 cm^{-3}, respectively, followed by summer (16.6×10^3 cm^{-3}) and minimized in autumn (13.9×10^3 cm^{-3}). This result is comparable to the previous measurements conducted in urban Taipei where the seasonal means of PNCs ($10 < d < 560$ nm) ranged from 11×10^3 to 17×10^3 cm^{-3} (Cheng et al., 2014). Figure 2 illustrates the number, surface and volume size distributions of the aerosol particles. The geometric mean diameter (GMD) of each PSD mode was retrieved from the data of number concentrations. It was found that the GMDs of the nucleation, Aitken and accumulation modes were 10.4–12.8 nm, 26.5–38.4 nm, and 91.8–159.0 nm, respectively.

It was revealed that the nucleation mode particles were predominant in the PNCs during autumn, winter and spring in this study area, whereas a distinct size distribution pattern was observed in summertime where the fraction of nucleation mode

ACPD
15, 21803–21835, 2015

(N_{4-25}/N_{4-736}) decreased to 0.44 and the Aitken mode PNCs increased to be comparable to that of the nucleation mode in summer. Observation from another aspect is that the PNC of nucleation mode (N_{4-25}) peaked in winter and minimized in summer, whereas the PNCs of Aitken mode (N_{25-100}) and accumulation mode ($N_{100-736}$) reached their respective maxima in summertime. Apparently, a large number of nucleation mode particles could have been shifted into the Aitken and/or accumulation modes in summer. The changes in the size distribution in summer season are most likely due to the seasonally enhanced photochemical production of condensable vapors that, in turn, will contribute to the growth of aerosol particles in the atmosphere. This seasonality agrees with our previous findings that the growth rate of newly formed particles was dominated by the photolysis of ozone, an indicator of photochemical activity (Cheung et al., 2013). The causes responsible for the observed seasonal variations in PNCs will be discussed in more details in following sections.

3.2 Mass concentration and chemical composition

Figure 3a and b illustrates the averaged chemical composition and mass concentration of UFPs and PM_1, respectively, for each season. Details of the mass concentration and chemical composition of UFPs and PM_1 are listed in Table S1 in the Supplement.

The seasonal means of UFPs range from 0.73 to 1.62 $\mu g\,m^{-3}$, with an annual average of 1.01 $\mu g\,m^{-3}$. The measured UFPs mass concentration of the present study is comparable to that in urban area of Los Angeles, United States which was 0.80–1.58 $\mu g\,m^{-3}$ (Hughes et al., 1998), and relatively higher than that in urban Helsinki, Finland (average: 0.49 $\mu g\,m^{-3}$, Pakkanen et al., 2001). For the chemical composition, organic carbon (OC) was found to be the major mass contributor, which accounted for 29.8 % (seasonal means ranging from 26.9 to 33.4 % for various seasons) of averaged mass concentration of UFPs, and elemental carbon (EC) was the second major component with averaged mass contribution of 5.1 % (2.4–7.6 %), followed by sulfate (SO_4^{2-}) at 4.3 % (3.4–6.4 %) and nitrite (NO_2^-) at 2.9 % (0.9–7.3 %). In addition, a large

ACPD
15, 21803–21835, 2015

fraction of mass was contributed by the group of "others", which consisted of mineral (K^+, Ca^{2+}, PO_4^{3-} and Mg^{2+}), sea-salt (Na^+ and Cl^-), and unidentified species. The results showed that, in average, mineral and sea salt components attributed only 3.5 % (ranging from 2.0–6.0 %) to UFPs mass concentration. Thus a substantial amount of UFPs remained unidentified, which was most likely relevant to the hydrogen and oxygen associated with organic carbon (OC). The conversion factors used to estimate the average molecular weight per carbon in particulate organic matter varied depending on the characteristic of aerosols. A lower factor value, 1.2, was usually suggested for saturated organic molecules, while higher value, 1.6, was adopted for water-soluble compounds which consist of multifunctional oxygenated groups, and even higher factor value was used for aged aerosols which contain higher portion of low and semi-volatile products of photochemical reactions (Turpin and Lim et al., 2001). The high fraction of the "others" group found in UFPs suggested that the photochemical production of secondary organic aerosols was a significant process responsible for the elevated UFPs levels observed in this study.

As shown in Fig. 3b, annual average of PM_1 was estimated to be 14.7 $\mu g\,m^{-3}$ (11.6–18.5 $\mu g\,m^{-3}$), which is similar to the results of a previous study in urban Taipei (average: 14.0 $\mu g\,m^{-3}$, Li et al., 2010). The measured PM_1 level was relatively higher than that of the urban areas of Phoenix, United States (5.9 $\mu g\,m^{-3}$, Lundgren et al., 1996) and Helsinki, Finland (6.1 $\mu g\,m^{-3}$, Vallius et al., 2000). For chemical composition, sulfate was the major mass contributor of PM_1 (average: 39.0 %, ranging from 33.8 to 46.8 %), followed by ammonium (average: 12.7 %, 12.0–13.2 %) and OC (average: 11.5 %, ranging from 9.2 to 14.3 %).

The results presented above indicate that UPFs exhibited distinct seasonality and composition from PM_1 in the study area. The highest UFPs concentration was observed in summer (1.62 $\mu g\,m^{-3}$) and the lowest in winter (0.73 $\mu g\,m^{-3}$). This result may be attributed to the stronger photochemical activities in summer which could have enhanced the formation of secondary organic aerosols. Consequently, the mass concentration of OC increased from 0.20 $\mu g\,m^{-3}$ in winter to 0.47 $\mu g\,m^{-3}$ in summertime. It

ACPD
15, 21803–21835, 2015

was noteworthy that the mass concentration of sulfate in UFPs also peaked in summer (64 ng m^{-3}), suggesting enhancement in photo-oxidation of SO_2. Cheung et al. (2013) found that photo-oxidation of SO_2 was the major mechanism for the formation of new particles in Taipei, Taiwan and the production of condensable vapors was also dominated by photo-oxidation. The co-variations in sulfate and OC revealed in this study further suggest that secondary organic compounds are the major condensable matter contributing to the growth of newly formed particles.

While the organics predominated in the mass concentration of UFPs, which included nucleation mode and Aitken mode particles, the measurements of PM_1 in this study suggest that sulfate was the major constituent of accumulation mode aerosols. In contrast to the seasonality of UFPs, the mass concentration of PM_1 reached the maximal at 18.5 µg m^{-3} in spring and exhibited the minimal at 11.6 µg m^{-3} in summer. The PM_1 differences between spring and summer were mostly due to declined ambient levels of sulfate, nitrate, and ammonium ions. As a result, the mass contribution of the three inorganic ions in PM_1 reduced from 55.7 to 46.2 % and, on the contrary, the mass fraction of OC increased from 10.2 to 14.3 %. The seasonal characteristics of PM_1 concentration and composition are attributed mostly to the changes in the origin areas of background air mass, which shifts from the Asia Continent to the western Pacific Ocean during summertime. Our previous studies reported that the fine particulate matter ($PM_{2.5}$) transported on the Asian outflows to northern Taiwan maximized in springtime and were enriched in sulfate, nitrate, and ammonium (Chou et al., 2008, 2010). The seasonality of PM_1 found in this study is consistent with the previous observations for $PM_{2.5}$ and thereby suggests the significance of Asian outflow aerosols to the PM_1 budget in the downwind areas of the Asia Continent.

3.3 Seasonal characteristics of photochemical production

In order to study the influences of photochemical production of particles, the measurements of PNC and PSD were analyzed per daytime (07:00–17:00 LT) and nighttime (17:00–07:00 LT), respectively (see Fig. 4). Since the particles in nighttime are mainly

ACPD
15, 21803–21835, 2015

emitted from the vehicular exhausts and the elevated PNCs in daytime are due to both the primary and secondary sources of the particles in the study area (Cheung et al., 2013), a larger difference between the PNCs observed in daytime and nighttime indicates stronger influence of photochemical production on the PNCs. The most striking seasonal features shown in Fig. 4 is the large difference between daytime against nighttime PSDs in summer as indicated by the low N_{4-736} (nighttime)/N_{4-736} (daytime) ratios, whereas higher ratios were observed in other seasons. This result is as expected because the photochemical production of nucleation mode particles was more intense during warm season in subtropical areas (Cheung et al., 2011). Moreover, as discussed in previous section, the photochemical reactions could produce condensable organics that allows the newly formed nucleation mode particles to grow into the Aitken mode. The relatively smaller differences between the daytime and nighttime N_{4-736} in autumn and winter show that the photochemical contribution in PNCs was declined as compared to that in summertime.

3.4 Influences of local emission on PNCs

Vehicle emission is known as the major source of the particulate matter in urban environment, particularly during the nighttime. In order to investigate the relationship between the vehicular exhausts and PNCs, the scatter plots of NO_x (as an indicator of vehicle emission) against N_{4-25}, N_{25-100} and $N_{100-736}$ during the nighttime were examined for winter and summer periods (see Fig. 5). The values of the Pearson correlation coefficient (r) and the slope of linear regression between NO_x and PNCs are summarized in Table 2.

The highest r values were found in both the plots of NO_x against N_{25-100} for winter (r = 0.88) and summer (r = 0.87). This result suggests that a strong linear correlation between the vehicle emission and the N_{25-100}, coincided with the results from previous studies (e.g., Morawska et al., 2008). During wintertime, stronger correlation was found between NO_x against N_{4-25} (r = 0.84) and N_{25-100} (r = 0.88) compared to that between NO_x and $N_{100-736}$ (r = 0.38). In contrast, high r values were obtained be-

ACPD
15, 21803–21835, 2015

tween NO_x and all particle modes in summer (r = 0.70–0.87). The robust correlation between NO_x and N_{4-25}/N_{25-100} suggests that local vehicle emission was the predominant source of UFPs throughout a year. However, in the winter case the PNCs of accumulation mode particles ($N_{100-736}$) were dominated by NO_x-independent sources, which was most likely relevant to the pollution outbreaks from the Asian continent. Lin et al. (2004) indicated that the long range transported air mass was characterized by high level of PM_{10} and low mixing ratio of NO_x due to its short atmospheric lifetime.

The slope values shown in Fig. 6 can serve as a relative emission factor of particles per NO_x in the study area, which indicates the degree of the influences of vehicle emission on the PNCs (Cheung et al., 2013). Relatively higher slope values found in summertime compared to winter period evidence a greater influence of the vehicle emission on particle concentration. Furthermore, the lower emission factor for nucleation mode and higher one for the Aitken mode demonstrate the size shift effects of particle growth in summer evening. The seasonal effects on the emission ratio of PNCs and NO_x are rather difficult to address since the complexity of different controlling factors, such as formation mechanisms and meteorological conditions. For example, Nam et al. (2010) reported negatively exponential correlation between the PM/NO_x ratio in vehicle emission and ambient temperature, and suggested that the impact of ambient temperature on particulate matter was larger than that on NO_x. Nevertheless, the observed differences in the $PNCs/NO_x$ ratios for winter and summer periods of this study necessitate further investigations on the formation mechanisms of aerosol particles in urban areas, in particular the nucleation and the Aitken modes.

3.5 Influence of long-range transport (LRT)

During the seasons of winter monsoons, i.e. from autumn to spring, the continental outflows have been frequently observed in urban Taipei, which is indicated by the stable northeasterly wind and increase of O_3 level (Lin et al., 2004). Previous studies of long-range transport (LRT) of air pollutants on air quality of northern Taiwan showed that an elevated PM_{10} was observed under the influence of continental outflows (Lin et al.,

ACPD
15, 21803–21835, 2015

2004; Chou et al., 2004). Figure 6 demonstrates an LRT pollution event observed at the TARO during this study. The wind direction changed from westerly/northwesterly to northeasterly at 21:00, 24 March and which continued until 06:00, 26 March. During this period, the O_3 mixing ratio remained at moderate level (~ 30–55 ppb) and PM_{10} increased from 10 to 98 $\mu g\,m^{-3}$. In this section, we attempt to analyze the PSDs/PNCs under the influences of continental pollution outbreaks. The periods of the respective LRT events are listed in Table S2 in the Supplement.

As shown in Fig. 6, the diurnal variations of PSD during the LRT event exhibited two N_{4-25} peaks associated to the morning and afternoon traffic rush hours, whereas the PNCs of the Aitken mode particles kept at a low level. This result suggests that the influences of local vehicle emission on PNCs were still in place, whereas growth of particles due to secondary production of condensable vapors could have been suppressed. The averaged PSDs for LRT and non-LRT cases are shown in Fig. 7. The geometric mean diameters of the nucleation, Aitken, and accumulation modes in PSDs were found to be at 10.6, 37.2 and 156.8 nm for LRT and 11.3, 30.0 and 113.4 nm for non-LRT cases, respectively. The median N_{4-25} ($11.1 \times 10^3\,cm^{-3}$), N_{25-100} ($7.3 \times 10^3\,cm^{-3}$) and $N_{100-736}$ ($1.8 \times 10^3\,cm^{-3}$) observed in non-LRT events are significantly higher than those for LRT events (N_{4-25}: $9.2 \times 10^3\,cm^{-3}$, N_{25-100}: $3.8 \times 10^3\,cm^{-3}$, $N_{100-736}$: $1.3 \times 10^3\,cm^{-3}$). This could be attributed to the lower wind speed (and hence poor dispersion) during non-LRT events ($1.5 \pm 0.8\,m\,s^{-1}$) than that for LRT events ($3.0 \pm 0.8\,m\,s^{-1}$). In contrast to the increases in PM_{10} observed usually during LRT episodes (e.g., Lin et al., 2012), the relatively lower PNCs suggest that the number concentration of submicron particles, in particular UFPs, are still dominated by local emissions during the episodes of continental pollution outbreaks. This is consistent with the observation of seasonal UFPs mass concentration that peaked in summertime when Taiwan was isolated from the influences of continental air mass.

ACPD
15, 21803–21835, 2015

3.6 Factors affecting new particle formation (NPF)

As shown in previous study, the NPF events were frequently observed in summer, which subsequently induced a notable increase in N_{4-25} in urban Taipei (Cheung et al., 2013). Figure 8a–d shows the scatter plots of N_{4-25} against NO_x for daytimes in each season. During the NPF events, a non-linear relationship between these two parameters was usually observed during the daytime (Cheung et al., 2013). The results show that remarkable NPF events were observed often in summer and occasionally in spring, but rarely in autumn and winter in the study area. The frequency of remarkable NPF events was found to be 8 out of 84 measurement days and the events were observed only in spring (3 out of 26 days) and summer (5 out of 14 days) seasons. The averaged particle growth and formation rates were found to be $4.3 \pm 0.8\,nm\,h^{-1}$ and $1.6 \pm 0.8\,cm^{-3}\,s^{-1}$, which were comparable to those measured in previous urban studies (e.g., Cheung et al., 2013). The particle growth and formation rates of each case are listed in Table S3 in the Supplement.

Table 3 summarizes the averages of N_{4-25}, PM_{10}, H_2SO_4 proxy (as UVB*SO_2/condensation sink) and wind speed for each season. The most significant factors relevant to the frequent particle formation observed in summertime are the low PM_{10} concentration ($35.6\,\mu g\,m^{-3}$) and high H_2SO_4 proxy (271.1 ppb W m^{-2} s) in the season. The association of sulfuric acid production and the NPF events agrees with the elevated mass concentration of sulfate in UFPs during summertime (shown in Table S1), as well as the results of previous urban studies (Woo et al., 2001; Cheung et al., 2013). This strongly supports that the new particle formation was mainly driven by the photochemical oxidation of SO_2 under low condensation sink conditions, where the SO_2 could be transported from the upwind area on the summer monsoons (see Fig. 1d). On the contrary, the absence of particle formation events in wintertime could be attributed to the suppression of NPF by particles transported from the Asian continent (Lin et al., 2004). The results of this work evidenced that low PM_{10}

ACPD
15, 21803–21835, 2015

concentration and high sulfuric acid production favor the particle formation process in urban areas.

4 Conclusions

The mass concentration and chemical composition of UFPs and submicron particles (i.e. PM_1) as well as the PNCs and PSDs with size ranged from 4 to 736 nm were measured during four seasonal campaigns in the period from October 2012 to August 2013 at the TARO, a subtropical urban aerosol station in East Asia. Significant differences in the seasonality and chemical composition of UFPs and PM_1 were revealed. The UFPs were composed mostly of organic matter and reached the maximal in summer, whereas the PM_1 composition was dominated by ammonium and sulfate and exhibited a seasonal peak in the spring.

It was found that the total PNCs in Taipei, Taiwan were elevated significantly during cold seasons, which were caused mostly by the high levels of nucleation mode particles (N_{4-25}). On the contrary, both the Aitken mode (N_{25-100}) and accumulation mode ($N_{100-736}$) PNCs reached their respective maxima in summertime. Consistent correlation without significant seasonal differences was found between the UFPs (i.e. nucleation and Aitken mode particles) and NO_x, suggesting that local vehicle emission is the major source of UFPs in the study area throughout a year. The local vehicle emission is also dominating the accumulation mode PNC in summer, but not in wintertime. The declined correlation between NO_x and $N_{100-736}$ in winter ($r = 0.38$) is likely due to the influences of air pollution associated with the Asian outflows.

The elevated UFPs level in summer is attributed to the increases in the concentration of Aitken mode particles (N_{25-100}). It was revealed from the measurements of PSD that a large number of nucleation mode particles could have shifted into the Aitken mode during summertime, which is most likely relevant to the photochemical production of condensable vapors that, in turn, could have contributed to the growth of particles in the atmosphere. Moreover, the chemical measurements suggest that the constituents

ACPD
15, 21803–21835, 2015

of the condensed materials in UFPs are mostly organic matter, underlining the significance of secondary organic aerosols in the ambient UFPs.

A total of 8 new particle formation (NPF) events occurred out of 84 measurement days in this study, which were observed in spring (3 events out of 26 days) and summer (5 events out of 14 days). The prevalence of NPF in summer agrees with the highest H_2SO_4 proxy and lowest PM_{10} observed in this study, which provided favorable atmospheric conditions for new particle formation. The averaged particle growth and formation rates for the NPF events are $4.3 \pm 0.8\,nm\,h^{-1}$ and $1.6 \pm 0.8\,cm^{-3}\,s^{-1}$, respectively, which are comparable to those measured in previous urban studies.

As exemplifying above, the characteristics of various physicochemical properties of particles investigated in this study and the occurrence of NPF exhibited a strong seasonality, which was co-influenced by the long-range transported particles during the seasons of winter monsoons and the strong photochemical activities in summer. The results of this study are critical for the authorities involved in urban development and health impact assessment, and the environmental policy makers who are tackling the severe atmospheric pollution in the East Asia region.

The Supplement related to this article is available online at doi:10.5194/acpd-15-21803-2015-supplement.

Acknowledgements. This research was supported by the Academia Sinica and the Ministry of Science and Technology of Taiwan through grants 103-2111-M-001-003, 102-2628-M-001-007, and 101-2119-M-001-003. The authors thank the Taiwan EPA for providing the air quality and meteorological data. We also thank the Department of Atmospheric Science of National Taiwan University for the logistical supports to the operation of TARO. Prof. Tareq Hussein is gratefully acknowledged for providing us the code of DO-FIT.

ACPD
15, 21803–21835, 2015

References

Charlson, R. J., Schwartz, S. E., Hales, J. M., Cess, R. D., Coakley Jr., J. A., Hansen, J. E., and Hofmann, D. J.: Climate forcing by anthropogenic aerosols, Science, 255, 423–430, 1992.

Cheng, Y.-H., Kao, Y.-Y., and Liu, J.-J.: Correlations between black carbon mass and size-resolved particle number concentrations in the Taipei urban area: a five-year long-term observation, Atmos. Pollut. Res., 5, 62–72, 2014.

Cheung, H. C., Wang, T., Baumann, K., and Guo, H.: Influence of regional pollution outflow on the concentrations of fine particulate matter and visibility in the coastal area of southern China, Atmos. Environ., 39, 6463–6474, 2005.

Cheung, H. C., Morawska, L., and Ristovski, Z. D.: Observation of new particle formation in subtropical urban environment, Atmos. Chem. Phys., 11, 3823–3833, doi:10.5194/acp-11-3823-2011, 2011.

Cheung, H. C., Chou, C. C.-K., Huang, W.-R., and Tsai, C.-Y.: Characterization of ultrafine particle number concentration and new particle formation in an urban environment of Taipei, Taiwan, Atmos. Chem. Phys., 13, 8935–8946, doi:10.5194/acp-13-8935-2013, 2013.

Chou, C. C.-K., Lin, C.-Y., Chen, T.-K., Hsu, S.-C., Lung, S.-C., Liu, S. C., and Young, C.-Y.: Influence of long-range transport dust particles on local air quality: a case study on Asian dust episodes in Taipei during the Spring of 2002, Terr. Atmos. Ocean. Sci., 15, 881–889, 2004.

Chou, C. C.-K., Huang, S.-H., Chen, T.-K., Lin, C.-Y., and Wang, L.-C.: Size-segregated characterization of atmospheric aerosols in Taipei during Asian outflow episodes, Atmos. Res., 75, 89–109, 2005.

Chou, C. C.-K., Lee, C.-T., Yuan, C. S., Hsu, W. C., Hsu, S. C., and Liu, S. C.: Implications of the chemical transformation of Asian outflow aerosols for the long-range transport of inorganic nitrogen species, Atmos. Environ., 42, 7508–7519, 2008.

Chou, C. C.-K., Lee, C. T., Cheng, M. T., Yuan, C. S., Chen, S. J., Wu, Y. L., Hsu, W. C., Lung, S. C., Hsu, S. C., Lin, C. Y., and Liu, S. C.: Seasonal variation and spatial distribution of carbonaceous aerosols in Taiwan, Atmos. Chem. Phys., 10, 9563–9578, doi:10.5194/acp-10-9563-2010, 2010.

Donaldson, K., Li, X. Y., and MacNee, W.: Ultrafine (nanometre) particle mediated lung injury, J. Aerosol Sci., 29, 553–560, 1998.

ACPD
15, 21803–21835, 2015

Draxler, R. R.: HYSPLIT4 user's guidem, NOAA Tech. Memo. ERL ARL-230, NOAA Air Resources Laboratory, Silver Spring, MD, USA, 1999.
Guo, H., Ding, A., Morawska, L., He, C., Ayoko, G., Li, Y., and Hung, W.: Size distribution and new particle formation in sub-tropical eastern Australia, Environ. Chem., 5, 382–390, 2008.
Holman, J. P.: Heat Transfer, McGraw-Hill, New York, USA, 1972.
Hsu, S.-C., Lee, C. S. L., Huh, C.-A., Shaheen, R., Lin, F.-J., and Liu, S. C.: Ammonium deficiency caused by heterogeneous reactions during a super asian dust episode, J. Geophys. Res., 119, 6803–6817, doi:10.1002/2013JD021096, 2014.
Hughes, L. S., Cass, G. R., Gone, J., Ames, M., and Olmez, I.: Physical and chemical characterization of atmospheric ultrafine particles in the Los Angeles area, Environ. Sci. Technol., 32, 1153–1161, 1998.
Hussein, T., Dal Maso, M., Petäjä, T., Koponen, I. K., Paatero, P., Aalto, P. P., Hämeri, K., and Kulmala, M.: Evaluation of an automatic algorithm for fitting the particle number size distributions, Boreal Env. Res., 10, 337–355, 2005.
Juwono, A., Johnson, G. R., Mazaheri, M., and Morawska, L., Roux, F., and Kitchen, B.: Investigation of the airborne submicrometer particles emitted by dredging vessels using a plume capture method, Atmos. Environ., 73, 112–123, 2013.
Kulmala, M.: How particles nucleate and grow, Science, 302, 1000–1001, 2003.
Kulmala, M., Vehkamäki, H., Petäjä, T., Dal Maso, M., Lauri, A., Kerminen, V.-M., Birmili, W., and McMurry, P. H.: Formation and growth rates of ultrafine atmospheric particles: a review of observations, J. Aerosol Sci., 35, 143–176, 2004.
Kulmala, M., Kontkanen, J., Junninen, H., Lehtipalo, K., Manninen, H. E., Nieminen, T., Petäjä, T., Sipilä, M., Schobesberger, S., Rantala, P., Franchin, A., Jokinen, T., Järvinen, E., Äijälä, M., Kangasluoma, J., Hakala, J., Aalto, P. P., Paasonen, P., Mikkilä, J., Vanhanen, J., Aalto, J., Hakola, H., Makkonen, U., Ruuskanen, T., Mauldin III, R. L., Duplissy, J., Vehkamäki, H., Bäck, J., Kortelainen, A., Riipinen, I., Kurtén, T., Johnston, M. V., Smith, J. N., Ehn, M., Mentel, T. F., Lehtinen, K. E. J., Laaksonen, A., Kerminen, V.-M., and Worsnop, D. R.: Direct observations of atmospheric aerosol nucleation, Science, 339, 943–946, 2013.
Lee, Y., Lee, H., Kim, M., Choi, C. Y., and Kim, J.: Characteristics of particle formation events in the coastal region of Korea in 2005, Atmos. Environ., 42, 3729–3739, 2008.
Li, C.-S., and Lin, C.-H.: PM_1 / $PM_{2.5}$/ PM_{10} characteristics in the urban atmosphere of Taipei, Aerosol Sci. Tech., 36, 469–473, 2010.

ACPD
15, 21803–21835, 2015

Lin, C.-Y., Liu, S. C., Chou, C. C.-K., Liu, T. H., and Lee, C.-T.: Long-range transport of Asian dust and air pollutants to Taiwan, Terr. Atmos. Ocean. Sci., 15, 759–784, 2004.

Lin, C.-Y., Chou, C. C.-K., Wang, Z., Lung, S.-C., Lee, C.-T., Yuan, C.-S., Chen, W.-N., Chang, S.-Y., Hsu, S.-C., Chen, W.-C., and Liu, S. C.: Impact of different transport mechanisms of Asian dust and anthropogenic pollutants to Taiwan, Atmos. Environ., 60, 403–418, 2012.

Lundgren, D. A. Hlaing, D. N., Rich, T. A., and Marlpe, V. A.: PM_{10}/ $PM_{2.5}$ PM_1 data from a trichotomous sampler, Aerosol Sci. Tech., 25, 353–357, 1996.

Matsumoto, K., Uyama, Y., Hayano, T., Tanimoto, H., Uno, I., and Uematsu, M.: Chemical properties and outflow patterns of anthropogenic and dust particles on Rishiri Island during the Asian Pacific Regional Aerosol Characterization Experiment (ACE-Asia), J. Geophys. Res., 108, 8666, doi:10.1029/2003JD003426, 2003.

Mazaheri, M., Johnson, G. R., and Morawska, L.: Particle and gaseous emissions from commercial aircraft at each stage of the landing and takeoff cycle, Environ. Sci. Technol., 43, 441–446, 2009.

Morawska, L., Ristovski, Z., Jayaratne, E. R., Keogh, D. U., and Ling, X.: Ambient nano and ultrafine particles from motor vehicle emissions: characteristics, ambient processing and implications on human exposure, Atmos. Environ., 42, 8113–8138, 2008.

Nam, E., Kishan, S., Baldauf, R. W., Fulper, C. R., Sabisch, M., and Warila, J.: Temperature effects on particulate matter emissions from light-duty, gasonline-powered motor vehicles, Environ. Sci. Technol., 44, 4672–4677, 2010.

Nie, W., Wang, T., Xue, L. K., Ding, A. J., Wang, X. F., Gao, X. M., Xu, Z., Yu, Y. C., Yuan, C., Zhou, Z. S., Gao, R., Liu, X. H., Wang, Y., Fan, S. J., Poon, S., Zhang, Q. Z., and Wang, W. X.: Asian dust storm observed at a rural mountain site in southern China: chemical evolution and heterogeneous photochemistry, Atmos. Chem. Phys., 12, 11985–11995, doi:10.5194/acp-12-11985-2012, 2012.

O'Dowd, C. D., McFiggans, G., Greasey, D. J., Pirjola, L., Hoell, C., Smith, M. H., Allan, B. J., Plane, J. M. C., Heard, D. E., Lee, J. D., Pilling, M. J., and Kulmala, M.: On the photochemical production of new particles in the coastal boundary layer, Geophys. Res. Lett., 26, 1707–1710, 1999.

Pakkanen, T. A., Kerminen, V.-M., Korhonen, C. H., Hillamo, R. E., Aarnio, P., Koskentalo, T., and Maenhaut, W.: Urban and rural ultrafine ($PM_{0.1}$) particles in the Helsinki area, Atmos. Environ., 35, 4593–4607, 2001.

ACPD
15, 21803–21835, 2015

Pérez, N., Pey, J., Cusack, M., Reche, C., Querol, X., Alastuey, A., and Viana, M.: Variability of particle number, black carbon, and PM_{10}, $PM_{2.5}$ and PM_1 levels and speciation: influence of road traffic emissions on urban air quality, Aerosol Sci. Tech., 44, 487–499, 2010.

Pey, J., Rodíguez, S., Querol, X., Alastuey, A., Moreno, T., Putaud, J. P., and Van Dingenen, R.: Variations of urban aerosols in the western Mediterranean, Atmos. Environ., 42, 9052–9062, 2008.

Pey, J., Querol, X., Alastuey, A., Rodiguez, S., Putaud, J. P., and Van Dingenen, R.: Source apportionment of urban fine and ultrafine particle number concentration in a Western Mediterranean city, Atmos. Environ., 43, 4407–4415, 2009.

Reche, C., Querol, X., Alastuey, A., Viana, M., Pey, J., Moreno, T., Rodríguez, S., González, Y., Fernández-Camacho, R., de la Rosa, J., Dall'Osto, M., Prévôt, A. S. H., Hueglin, C., Harrison, R. M., and Quincey, P.: New considerations for PM, Black Carbon and particle number concentration for air quality monitoring across different European cities, Atmos. Chem. Phys., 11, 6207–6227, doi:10.5194/acp-11-6207-2011, 2011.

Salvador, C. M. and Chou, C. C.-K.: Analysis of semi-volatile materials (SVM) in fine particulate matter, Atmos. Environ., 95, 288–295, 2014.

Subramanian, R., Khlystov, A. Y., Cabada, J. C., and Robinson, A. L.: Positive and negative artifacts in particulate organic carbon measurements with denuded and undenuded sampler configurations, Aerosol Sci. Tech., 38, 27–48, 2004.

Turpin, B. J. and Lim, H.-J.: Species contributions to $PM_{2.5}$ mass concentrations: revisiting common assumptions for estimating organic mass, Aerosol Sci. Tech., 35, 602–610, 2001.

Vallius, M. J., Ruuskanen, J., Mirme, A., and Pekkanen, J.: Concentrations and estimated soot content of PM_1, $PM_{2.5}$ and PM_{10} in a subarctic urban atmosphere, Environ. Sci. Technol., 34, 1919–1925, 2000.

Vehkamäki, H., Dal Maso, M., Hussein, T., Flanagan, R., Hyvärinen, A., Lauros, J., Merikanto, P., Mönkkönen, M., Pihlatie, K., Salminen, K., Sogacheva, L., Thum, T., Ruuskanen, T. M., Keronen, P., Aalto, P. P., Hari, P., Lehtinen, K. E. J., Rannik, Ü, and Kulmala, M.: Atmospheric particle formation events at Värriö measurement station in Finnish Lapland 1998-2002, Atmos. Chem. Phys., 4, 2015–2023, doi:10.5194/acp-4-2015-2004, 2004.

Wang, T., Ding, A. J., Blake, D. R., Zahorowski, W., Poon, C. N., and Li, Y.-S.: Chemical characterization of the boundary layer outflow of air pollution to Hong Kong during February–April 2001, J. Geophys. Res., 108, 8787, doi:10.1029/2002JD003272, 2003.

ACPD
15, 21803–21835, 2015

Weber, R. J., Moore, K., Kapustin, V., Clarke, A., Mauldin, R. L., Kosciuch, E., Cantrell, C., Eisele, F., Anderson, B., and Thornhill, L.: Nucleation in the equatorial pacific during PEM-tropics B: enhanced boundary layer H_2SO_4 but no particle production: NASA global tropospheric experiment Pacific Exploratory Mission in the tropics phase B, Part 1: Measurement and analyses (PEM-Tropics B), J. Geophys. Res., 106, 32767–32776, 2001.

Woo, K. S., Chen, D. R., Pui, D. Y. H., and McMurry, P. H.: Measurement of Atlanta aerosol size distribution: observation of ultrafine particle events, Aerosol Sci. Tech., 34, 75–87, 2001.

ACPD
15, 21803–21835, 2015

Table 1. Median and standard deviation of the PNCs measured in each season. The size ranges of the PNCs are represented by the subscripted number. For example, N_{4-25}, represents the number concentrations of the particles from 4 to 25 nm.

	Measurement periods	N_{4-736} (#/cm^3)	N_{4-25} (#/cm^3)	N_{25-100} (#/cm^3)	N_{4-100} (#/cm^3)	$N_{100-736}$ (#/cm^3)	N_{4-25}/N_{4-736}	N_{4-100}/N_{4-736}
Autumn	24 Oct–15 Nov 2012	13.9×10^3 (6.7×10^3)	8.6×10^3 (4.5×10^3)	3.9×10^3 (2.7×10^3)	12.7×10^3 (6.4×10^3)	1.3×10^3 (0.9×10^3)	0.62	0.90
Winter	4–24 Jan 2013	17.4×10^3 (8.7×10^3)	11.6×10^3 (6.0×10^3)	4.1×10^3 (3.7×10^3)	16.3×10^3 (8.5×10^3)	0.9×10^3 (0.9×10^3)	0.70	0.94
Spring	17 Mar–11 Apr 2013	19.4×10^3 (13.8×10^3)	10.3×10^3 (11.3×10^3)	5.8×10^3 (4.3×10^3)	17.0×10^3 (13.6×10^3)	1.9×10^3 (1.1×10^3)	0.56	0.89
Summer	1–14 Aug 2013	16.6×10^3 (16.4×10^3)	6.9×10^3 (9.1×10^3)	6.0×10^3 (9.1×10^3)	13.7×10^3 (15.4×10^3)	3.1×10^3 (2.6×10^3)	0.44	0.87

ACPD
15, 21803–21835, 2015

Table 2. Pearson correlation coefficient (r) and slope of linear regression of PNCs against NO_x during the nighttime (20:00–04:00 LT) in winter and summer periods.

Periods		N_{4-25}	N_{25-100}	$N_{100-736}$
Winter	Slope	279	163	18
	r	0.84	0.88	0.38
Summer	Slope	239	330	155
	r	0.76	0.87	0.70

ACPD
15, 21803–21835, 2015

Table 3. Median of N_{4-25}, PM_{10}, $UVB^{*}SO_2$, H_2SO_4 proxy and wind speed of different seasons.

Periods	N_{4-25} (cm^{-3})	PM_{10} ($\mu g\,m^{-3}$)	$UVB^{*}SO_2$ ($ppb\,W\,m^{-2}$)	H_2SO_4 proxy ($ppb\,W\,m^{-2}\,s$)	Wind speed ($m\,s^{-1}$)
Autumn	8.6×10^3	53.9	2.46	75.2	2.82
Winter	11.6×10^3	48.4	2.24	113.2	2.34
Spring	10.5×10^3	61.1	3.01	67.8	2.17
Summer	6.9×10^3	35.6	7.28	271.1	2.35

* The data with observation of rainfall was not used in calculation.

ACPD
15, 21803–21835, 2015

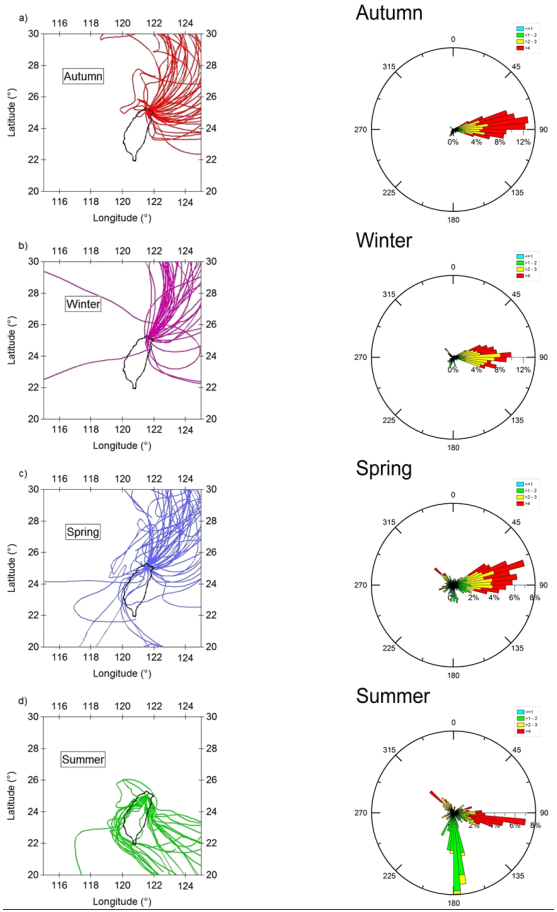

Figure 1. Back-trajectories calculated for TARO for the measurement periods (left panel) and surface wind rose plots (right panel) in **(a)** autumn, **(b)** winter, **(c)** spring and **(d)** summer.

ACPD
15, 21803–21835, 2015

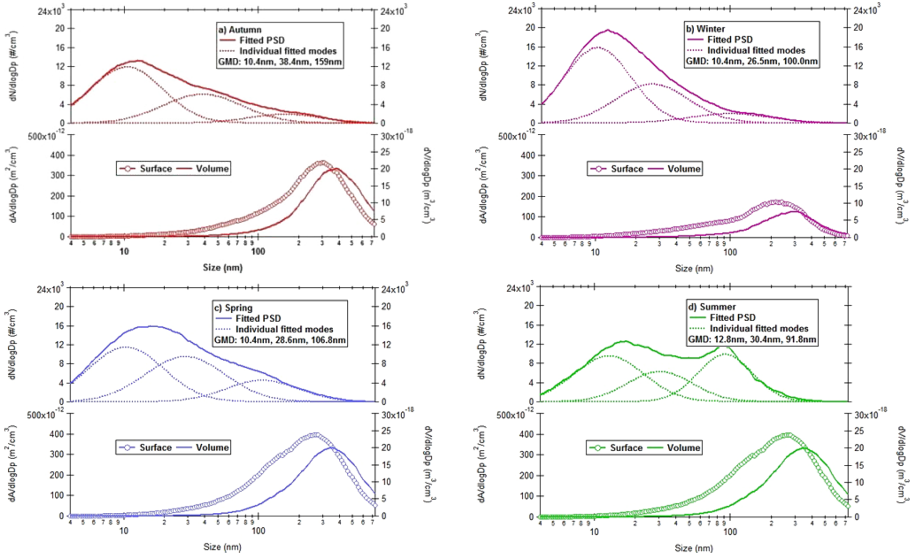

Figure 2. Size distribution of particle number (upper panel), surface and volume (lower panel) concentrations measured in **(a)** autumn, **(b)** winter, **(c)** spring and **(d)** summer (by curve fitting).

ACPD
15, 21803–21835, 2015

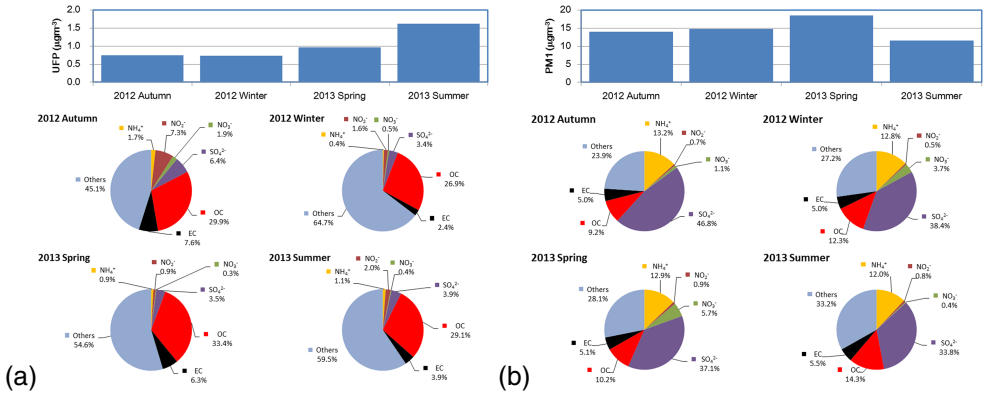

Figure 3. Seasonal concentration and composition of **(a)** ultra-fine (UFPs) and **(b)** sub-micron (PM_1) particles observed at the TARO in Taipei, Taiwan from autumn 2012 to summer 2013.

ACPD
15, 21803–21835, 2015

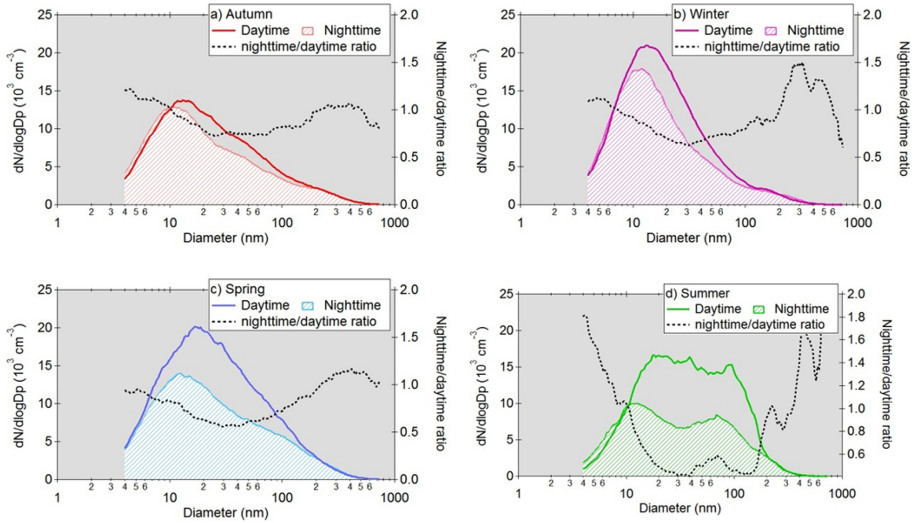

Figure 4. Median PSDs measured during the daytime (07:00–17:00 LT) and nighttime (17:00–07:00) in **(a)** autumn, **(b)** winter, **(c)** spring and **(d)** summer.

ACPD
15, 21803–21835, 2015

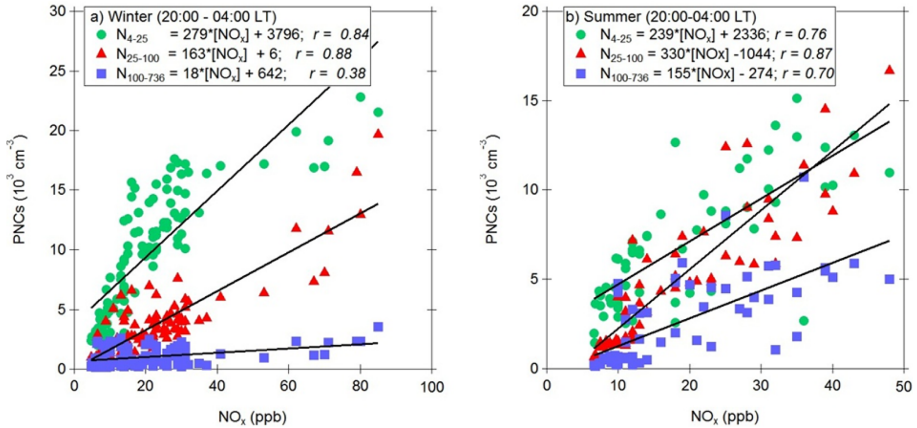

Figure 5. Scatter plots for PNCs vs. NO_x measured during the time period of 20:00–04:00 (LT) in **(a)** winter and **(b)** summer, with classification of various particle size ranges.

ACPD
15, 21803–21835, 2015

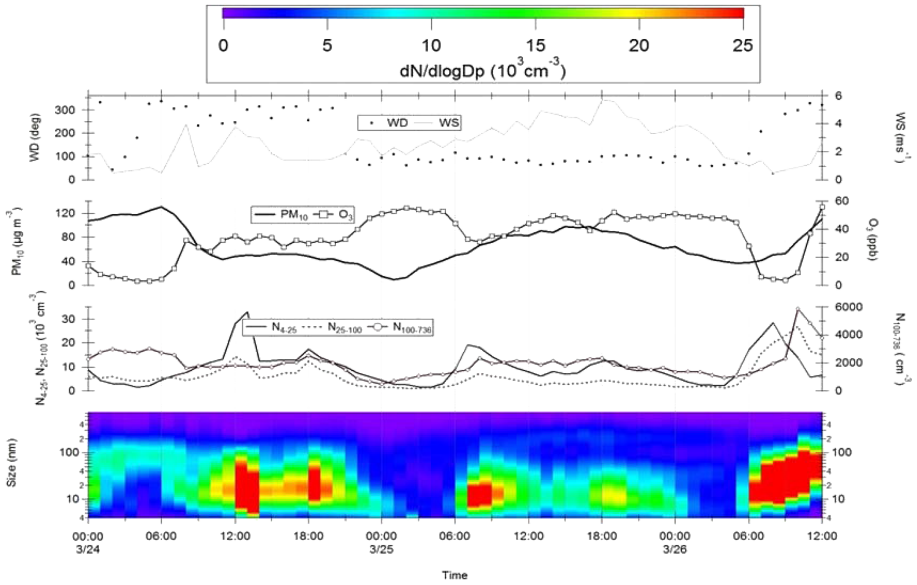

Figure 6. Time series of PSD, the N_{4-25}, N_{25-100}, $N_{100-736}$, PM_{10}, ozone (O_3) and wind direction/speed measured from 24–26 March 2013 (from bottom to top).

ACPD
15, 21803–21835, 2015

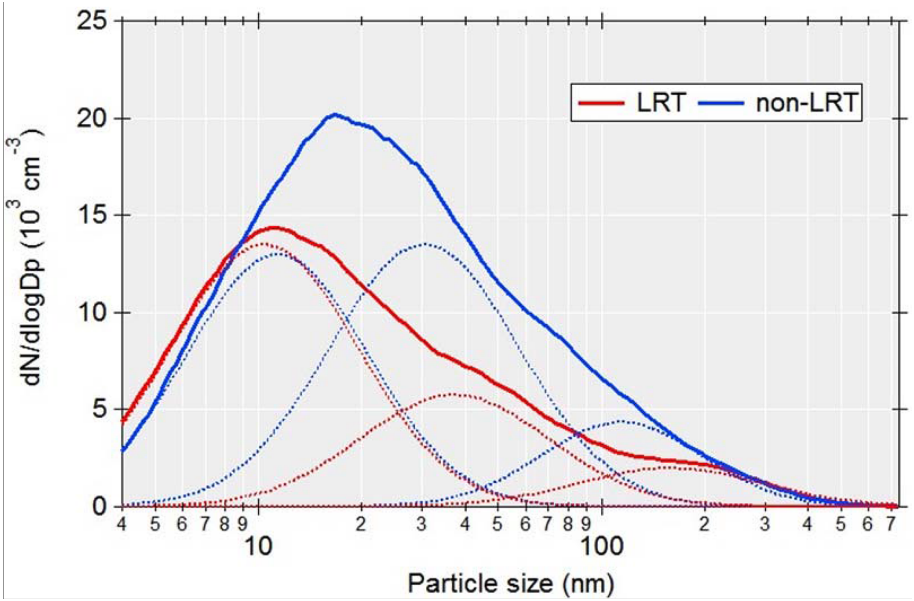

Figure 7. Averaged PSDs for LRT and non-LRT episodes measured during the seasons of winter monsoons. Dashed lines illustrate the PSD of each individual mode.

ACPD
15, 21803–21835, 2015

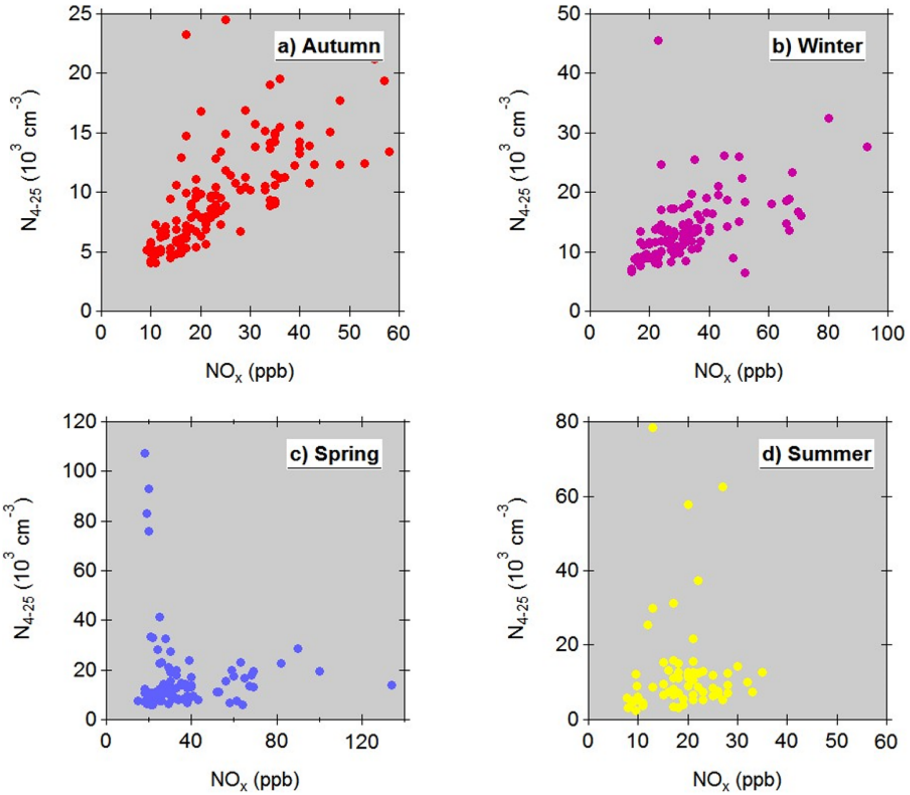

Figure 8. Scatter plots between N_{4-25} and NO_x observed in **(a)** Autumn, **(b)** Winter, **(c)** Spring and **(d)** Summer at TARO site during the period of 07:00–17:00 LT.

ACPD
15, 21803–21835, 2015